Medicinal Chemistry Research (2019) 28:160–168
https://doi.org/10.1007/s00044-018-2273-y

MEDICINAL CHEMISTRY RESEARCH

ORIGINAL RESEARCH

Controlled release of losartan from acid- and heat-treated halloysite nanotubes

Farid Moeinpour[1] · Faezeh Soofivand[2] · Fatemeh S. Mohseni-Shahri[1]

Received: 15 September 2018 / Accepted: 4 December 2018 / Published online: 12 December 2018

Abstract

In this work, a simple method was used to sustained release of losartan (LOS) as a high blood pressure-controller drug using halloysites (HNT) as a carrier. The present work can be considered as an effective method because of using HNT as a natural source, which is available, inexpensive, safe with specific structure that led to release of drug, gradually. This carrier was improved by calcination and etching processes and their effect was investigated on loading amount and in vitro release of drug from HNT. The products were characterized by various analyses such as: BET (Brunauer–Emmett–Teller), TG (thermal gravimetry), TEM (transmission electron microscopy), and XRD (X-ray powder diffraction). According to the studies, two processes improving had no effect on structure and morphology of HNT and only increased the lumen size of them. It should be noted, removal water molecules through calcination had binary effect on halloysites: enlargement of lumen and decreasing the drug loading. Besides, release rate was investigated and it showed that maximum and minimum release rate of LOS are assigned to simple HNT and etched-HNT (EHNT), respectively. Kinetics studies confirmed that releasing the LOS molecules from HNT followed by diffusion process that is identified as Fickian diffusion.

Keywords Halloysite · Losartan · Drug-delivery · Etching · Calcination · Diffusion and release

Introduction

Losartan (2-butyl-4-chloro-1-[[2′-(1H-tetrazol-5-yl)[1,1′-biphenyl]-4-yl]-methyl]-1H- imidazole-5-methanol; LOS) is used to treat high blood pressure and to assist in protecting the kidneys from breakdown owing to diabetes. It is also used in pulling down the danger of strokes in patients with high blood pressure. LOS is located in a class of drugs called angiotensin receptor blockers. It operates by relaxing blood vessels so that blood can flow more comfortably. LOS is well absorbed following oral administration. Prescription of formal tablets of LOS may exhibit variation in the plasma drug levels, resulting either in apparition of side-effects and decrease in drug concentration at the receptor site. Therefore, studies on adjustment of drug release by formulating its controlled release system (Patel 2010; Raju et al. 2010; Chithaluru et al. 2011; Sarwar and Hossain 2012), would be beneficial as it would reduce the side effects and improve patient satisfaction.

Nanoscale drug delivery is a novel technique for prevailing the aforesaid problems. These systems are new technologies for the efficient delivery of chemotherapeutic drugs in the treatment of diseases mostly cancers. Nanoparticles are used for site-specific drug delivery. They improve drug bioavailability. Bioavailability is defined as availability of a drug at target site. It depends on route of administration, rate of absorption, and metabolism of the drug by the body. Nanoscale delivery systems can be used to upgrade current treatment systems such as (i) targeting, enhancement of the drug concentration at required sites of action, and reduce systemic levels of the drug and its toxic effects in healthful tissues, (ii) enhanced solubility, to make easier parenteral drug provision (Hoffman 2008), (iii) reduced release, to increase the drug half-life, and (iv) increased drug stability, to reduce decay and maximize drug affection (Xin et al. 2016). Bioavailability of drugs may be

Supplementary information The online version of this article (https://doi.org/10.1007/s00044-018-2273-y) contains supplementary material, which is available to authorized users.

✉ Farid Moeinpour
fmoeinpour52@iauba.ac.ir

[1] Department of Chemistry, Bandar Abbas Branch, Islamic Azad University, Bandar Abbas 7915893144, Iran

[2] Young Researchers and Elite Club, Bandar Abbas Branch, Islamic Azad University, Bandar Abbas, Iran

less. Sometimes drug delivery may lead to over dosage toxicity and consequential inflammatory response. Therefore, targeted drug delivery aims to deliver the right of amount of drug at only the site of disease or injury (Zhang et al. 2017). Nanoscale drug delivery methods are available as nanocapsules (Xin et al. 2017), liposomes (Alavi et al. 2017), nanoparticles (Baeza et al. 2017), and microemulsions (Callender et al. 2017). Within this subject, natural existing HNT nanotubes (HNTs, ca. 1 μm in length and 80 nm in diameter) are fascinating a great scientific interest owing to the special hollow tubular shape (Lvov et al. 2008; Lvov and Abdullayev 2013). HNTs are two-layered aluminosilicates with chemical composition analogous to kaolin (Zhang et al. 2012; Pan et al. 2014), but differ in having a hollow tubular structure. In comparison with other nano-sized materials, e.g., carbon nanotubes, HNTs ($Al_2Si_2O_5(OH)_4{\cdot}nH_2O$) are easily attainable, much less expensive, and have peculiar structures (Pan et al. 2011). The external surface is constituted of Si−O−Si groups and the internal surface of a gibbsite-like collection of Al−OH groups. The particular surface chemistry permits the selective functionalization at the inner or outer side (Cavallaro et al. 2012; Yah et al. 2012; Cavallaro et al. 2013). HNT cytocompatibility was manifested (Vergaro et al. 2010), and its usage as a drug carrier was suggested (Viseras et al. 2008; Vergaro et al. 2012). Because of the high level of biocompatibility and low cytotoxicity of HNTs, these materials have been greatly studied for possible biomedical usages such as controlled drug-delivery systems, stem cell attachments and multiplication, and nanoreactors for enzymes immobilization (Cavallaro et al. 2015; Li et al. 2015; Kadam et al. 2017; Kerdsakundee et al. 2017; Nie et al. 2017). In last years, the functionalization of HNT by different procedures involving acid-activation (White et al. 2012), intercalation (Nicolini et al. 2009), thermo-chemical treatment, and chemical modification (Mu et al. 2008) has fascinated significant interests to make better properties of HNT and its performance. In general terms, acid treatment will lead to disaggregation of HNT particles, elimination of mineral impurities, and even dissolution of the inner layers. The lumen of HNT nanotube could been enlarged by selectively etching of alumina from the inner wall using sulfuric acid according to the report of Abdullayev et al. (2012). The structure of HNT was destroyed and the surface activity was improved after acid-treatment at 90 °C (Zhang et al. 2012). Heat activation can remove the physically bounded water, demolish the structure water through dehydroxylation of the structural aluminol groups and result in the structural rearrangement of HNT, which correspondingly alters the pore structure and surface properties (Kadi et al. 2012). Therefore, the adsorption properties of HNT were affected with the changes of its physicochemical properties. Up to now, acid- and heat-activated HNT samples were mainly used as adsorbents for dyes and metal ions. However, little information can be seen concerning the effects of acid- and heat treatments of HNT on its release property for drugs although HNT is a well-known promising carrier for drug delivery. In this work, the effects of acid- and heat-treatments on structure and morphology of HNT, its sustained-release properties for LOS were studied. To study the effect of preparation processes on the performance of HNTs, HNTs were improved by calcination and etching. According to the findings, these processes both increase the lumen size of HNT but calcination decreases the amount of drug-loading and increases the release rate compared with EHNT, owing to removal of water molecules, which affect the performance of carrier, severely. Besides, reaction of H^+ with aluminol groups existed in internal surfaces of HNTs led to sustained release and provided the best performance. So that, the release rate of it was only ~ 52.5 % after 70 h.

Materials and methods

Materials

Halloysite clay was supplied by naturalnano-US. LOS was supplied by Abidi Pharmaceutical Co., Ltd (Islamic republic of IRAN). Other agents used were all of analytical grade and all solutions were prepared with distilled water.

Etching process of HNTs

The etching process of HNT was carried out as follows: 1.0 g of HNT powder was added to the 500 mL of aqueous solution of H_2SO_4 2 M (mol L^{-1}) at room temperature and the mixture was stirred at 90 °C for 6 h. Next, in order to naturalize the pH of solution, it was washed by distilled water, several times. Then, white-color product was dried in vacuum oven at 90 °C and was branded as EHNT.

Calcination process of HNTs

According to the TG analysis, HNT structure is stable until 400 °C (Wang et al. 2014). So, in this work calcination temperature was adjusted at 400 °C. In total, 1.0 g of HNT powder was put in furnace and heated at this temperature for 2 h. Then, product was cooled to room temperature and was identified as CHNT.

Loading process of LOS in HNTs

In typical process, drug loading is done as follows: a supersaturated solution of drug was prepared, then HNT was added to it and the mixture was alternately vacuumed for 2

h during the certain periods as 20 min in vacuum and 10 min in atmosphere pressure. By considering the high solubility of LOS in water ($>500\ mg\ mL^{-1}$), super-saturated solution of LOS was prepared in ethanol (solubility of LOS in ethanol $=>20\ mg\ mL^{-1}$). Entrance of drug to HNTs induced by capillarity force that is owing to their hollow cylindrical structures in the presence of polar liquids (Wei et al. 2014). Besides, electrostatic interactions between inner surfaces of HNTs (positive charge of alumina groups) with negative charge of LOS can be considered as another agent for conjugation of LOS with HNTs.

In vitro release tests

The drug release kinetics of LOS-loaded HNTs were measured under a static release condition using the dialysis bag technique. About 0.5 g of LOS-loaded HNTs was placed in a dialysis bag. The dialysis bag was immersed into 25 mL of buffer solution (pH = 7.4) at 37 °C under magnetic stirring. At different time intervals, buffer samples were collected, replaced with fresh buffer, and the concentration of desorped LOS was determined by UV–vis in the withdrawn samples. UV–vis evaluation of LOS was done at 232 nm. The tests were carried out in triplicate, and the results were recorded as an average. Cumulative LOS release (%) was calculated as follows:

$$\text{Cumulative release rate}\ (\%) = \frac{M_t}{M_0} \times 100 \quad (1)$$

where M_t is the amount of LOS released from the HNTs at time t and M_0 is the amount of LOS initially loaded onto the HNTs.

The kinetics of the LOS released from HNT samples was determined by fitting the release profiles to the following theoretical models:

First order model:

$$f_t = 1 - e^{-k_1 t} \quad (2)$$

where f_t is the portion of drug dissolved in time t, and k_1 is the first order release constant.

Higuchi model:

$$f_t = k_H t^{0.5} \quad (3)$$

Where k_H is the Higuchi release constant.

Power law model:

$$f_t = k_p t^n \quad (4)$$

Where k_p is the release constant; n is the diffusion exponent, property of the release mechanism.

Characterization of HNTs

The crystalline phase of the HNT, CHNT, and EHNT were analyzed using a diffractometer of the Philips Company with X'Pert Promonochromatized Cu Kα radiation ($\lambda =$ 1.54 Å). Transmission electron microscopy (TEM) was conducted using a LEO 912AB Zeiss electron microscope (Germany) at 120 kV to describe the shape and structure of HNT nanotubes. Nitrogen adsorption–desorption isotherms studies were performed on an Autosorb-1 Quantachrome-Sorptometer (USA). The surface areas were calculated using the Brunauer–Emmett–Teller (BET) method and the pore size distribution and pore volume were calculated using the Barrett–Joyner–Halenda (BJH) method. Thermogravimetric analyses (TGA) were performed from 30 to 900°C (heating rate of 10°C/min) under air flow, using a Mettler TC-10 thermo-balance.

Statistical analysis

Statistical analysis for the determination of differences in the release properties within groups was performed by one-way analysis of variance, executed with a statistical program (Origin 5.0). The data were considered to be meaningfully different at $p < 0.05$. All data are presented as mean values with standard error (mean ± SD).

Results and discussion

Characterization and physicochemical aspects

Figure 1a–c illustrates the N_2 adsorption–disorption isotherms of HNT, EHNT, and CHNT, before loading, respectively. According to the IUPAC classification, these isotherms are type II and hysteresis loops are H3. These characteristics are indicator of meso- and macro pores structures. The results were summarized in Table 1. As shown, the maximum and minimum BET-specific surface area are related to the EHNT and HNT, respectively. As expected, etching process increases the lumen size during three steps as follows: infiltrating of H^+ ions to inner tube, reaction of these ions with alumina that exists on inner lumen and exodus of the produced products (Abdullayev et al. 2012). Also, insignificant increase of BET surface area and pore size of CHNT compared with HNT can be induced by dehydration of HNT during the calcination process.

Pore size distribution curves of HNT, EHNT, and CHNT determined from desorption branch of the N_2 isotherm using Barret–Joyner–Halenda (BJH) method are shown in Fig. 2a–c, respectively. These curves represent three index peaks at 3, 25, and ~ 78 nm, approximately.

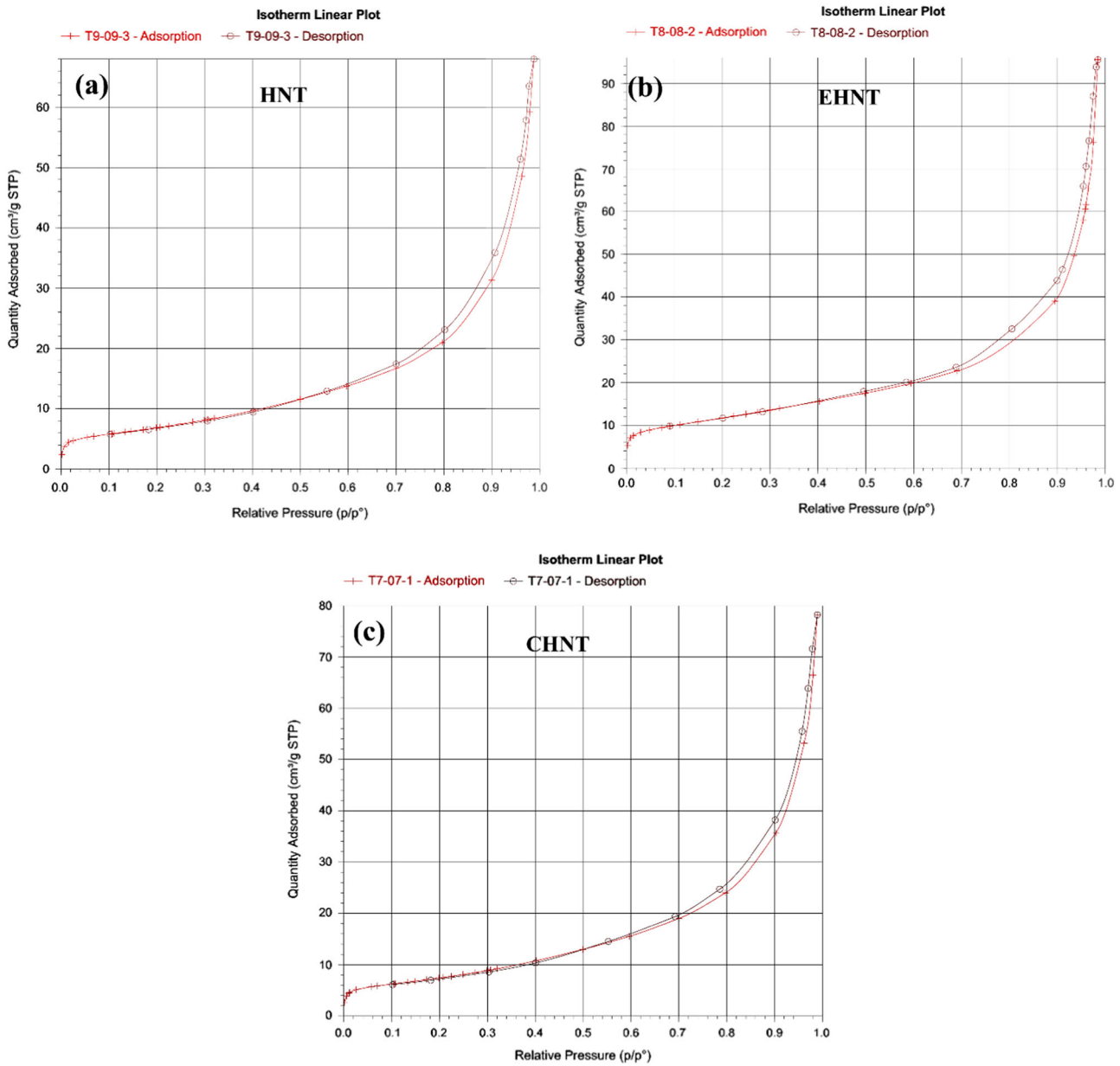

Fig. 1 The nitrogen adsorption–desorption isotherm of **a** HNT, **b** EHNT, and **c** CHNT

Table 1 Collection of the data of BET analysis, briefly

Characteristics (m^2/g)	HNT	EHNT	CHNT
BET surface area (m^2/g)	25.288	42.2049	27.5292
BJH desorption volume (1.7–300 nm) (m^2/g)	0.1058	0.1476	0.1218
Pore volume (cm^3/g)	0.0742	0.0976	0.0806

The low-width hysteresis loops at relative pressure $(P/P_0) > 0.4$ confirmed the broad pore size distribution from meso- to macro pores in these samples (Wang et al. 2014). According to that reported in the previous works, 3.5 nm meso-pores with slit-shaped longitudinal structures can be formed by dehydration of HNTs or tensile strength effect (Groen et al. 2003; Tan et al. 2013). In fact, these pores are artificial pores that are created during preparation process of HNT. The other meso-pores are the lumens of HNTs. As expected, etching process can be effective on lumen pores as it increases the distribution particle size and intensity of these pore sizes.

To evaluate the amount of loaded drug into HNTs, TGA analysis was used. Figure 3a–c shows the TGA curves of HNT, EHNT, and CHNT loaded by drug, respectively. In all of curves, a continuous mass loss is shown at range 275–800 °C that is including: mass loss of HNT at 475–575 °C (Hemmatpour et al. 2015) and mass loss of LOS potassium

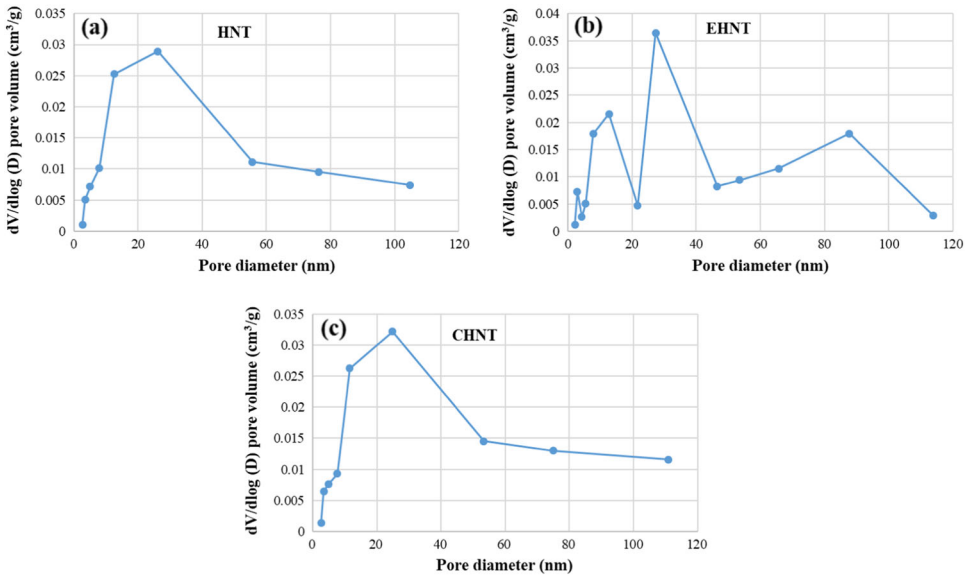

Fig. 2 The pore size distribution of **a** HNT, **b** EHNT, and **c** CHNT

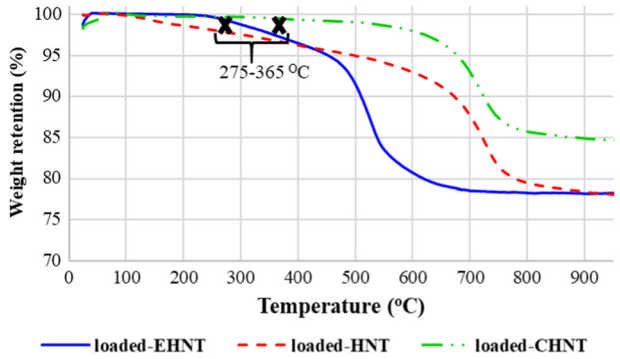

Fig. 3 TGA results of **a** HNT, **b** EHNT, and **c** CHNT

at 275–860 °C during the three steps: 275–365, 365–535, and 535–860 °C (M. Ibrahim 2015). So, loss mass at 275–365 °C is just related to LOS, which removes C_5H_8NCl. By considering the ref., mass loss % of losartanat the first step is ~25.2, therefore the drug percent into the HNT, EHNT, and CHNT were approximately calculated as 4, 8, and 2%, respectively. The slope of loss mass in these curves at $T = 275–365$ °C are dependent on the loaded-drug amount, the more drug the shaper slope. As shown, the maximum loading of drug is assigned to EHNT that the lumen size and the capacity of them increased by etching process. It was assued that the calculated drug content into HNTs is accordance with the lumen size of them. But the results illustrated that inspite of the bigger lumen size in CHNT, loaded-drug amount of it is lower than HNT. During calcination process, HNTs are dehydrated and the interlayer water molecules that play the main role for intercalation of HNTs are removed (Tan et al. 2013). So, the least drug was loaded into CHNT.

The results of TGA of the HNT and EHNT after loading were in agree with the results of BET analyses of them before loading. According to the results of both of analyses, the more drug was loaded in EHNT because of having the maximum BET surface area, volume, and size of pores. However, the minimum BET surface area and V and size of pores was assigned to HNT but the least drug was loaded in CHNT because of removal of intercalation agent that is interlayer water molecules. So, the presence of drug into HNTs was proved by the results of TG analyses.

XRD patterns of HNT, EHNT, and CHNT in two states: before and after drug loading were illustrated in Fig. 4a–f. The simple HNTs have two main peaks at $2\theta = 12$, 24.9 that the first is known as dehydrated peak of HNT, which is assigned to the reflection peak with miller index (0 0 1) with $d = 0.74$ nm and the latter confirms it (Wang et al. 2014). LOS potassium is identified by four peaks at about $2\theta =$ 10.8, 13.6, 20, and 24.2 in XRD pattern (Mokale et al. 2014). The other peaks can be assigned to calcite and quartz that was considered as impurities. As seen, peak positions of HNT and drug is very close and the distinction of them is difficult. Loading of drug had no obvious effect on intensity of peaks of HNT after loading compared with before loading because of the ratio of drug to HNT is low. As shown, the crystallinity of HNTs after loading has been increased that is due to the presence of drug into them. Furthermore, the effect of etching and calcination processes were investigated on XRD pattern of HNTs. The results showed that XRD pattern and crystallinity of EHNT is same as XRD pattern and crystallinity of HNT in the similar condition but they are different with CHNT. Calcination process removes the coordinated water of HNT, so the intensity of XRD peaks and crystallinity of calcined HNT is more than the others. Actual graphs of XRD have been provided in Fig. S1–A, B, C, D, E, and F from supplementary information.

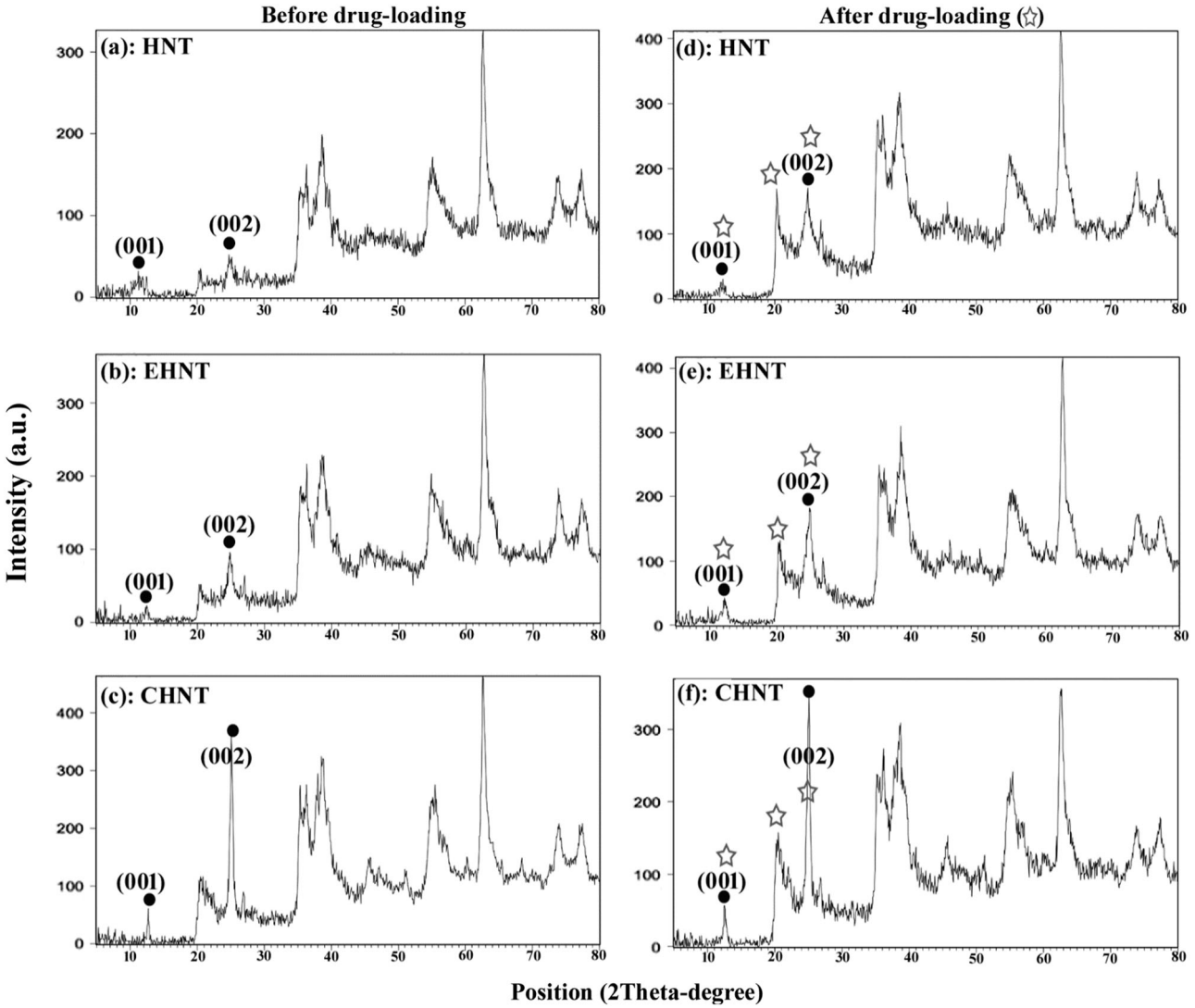

Fig. 4 XRD patterns of **a** HNT, **b** EHNT, **c** CHNT before loading and **d** HNT, **e** EHNT, **f** CHNT after loading, respectively

Figure 5a–c displays the TEM image of HNT, EHNT, and CHNT, respectively. These images obviously show the cylindrical structures with hollow centers that are parallel to outer cylinder structures. These structures are open-ended and the inner hollow cylinder is known as lumen. The effects of calcination and etching processes on morphology, size, and structure of HNTs were studied. The dimensions of HNTs was determined by Digimizer software. According to Fig. 5a, diameter of outer cylinder and size of lumen were estimated ~113.2 nm and 25.26 nm, respectively. As seems, these amounts were changed by calcination and etching processes. As shown in Fig. 5b, c, the lumen sizes of EHNT and CHNT are ~62.7 nm and 28.57, respectively. As expected, the lumen size of EHNT is more than the others because of etching process removes alumina molecules forming the inner surface of HNTs. On the other sides, HNT dehydrated by elimination of coordinated water molecules during the calcination process, so the size of lumen of CHNT becomes more than the simple HNT. These images indicated that calcination and etching processes have no significant effect on morphology of HNTs and the structure of them are maintained. These findings are agreement with the results of pore size distribution concluded from analyses.

The TGA results illustrated that the drug contents in EHNT is more than the other. So it can be concluded that drug-loading in HNTs is followed by various parameters and lumen size is not the only effective parameter.

In vitro release of LOS from HNTs

The release profiles of all three loaded HNT samples are shown in Fig. 6. As can be seen, the cumulative release rates in EHNT show significant differences with HNT and

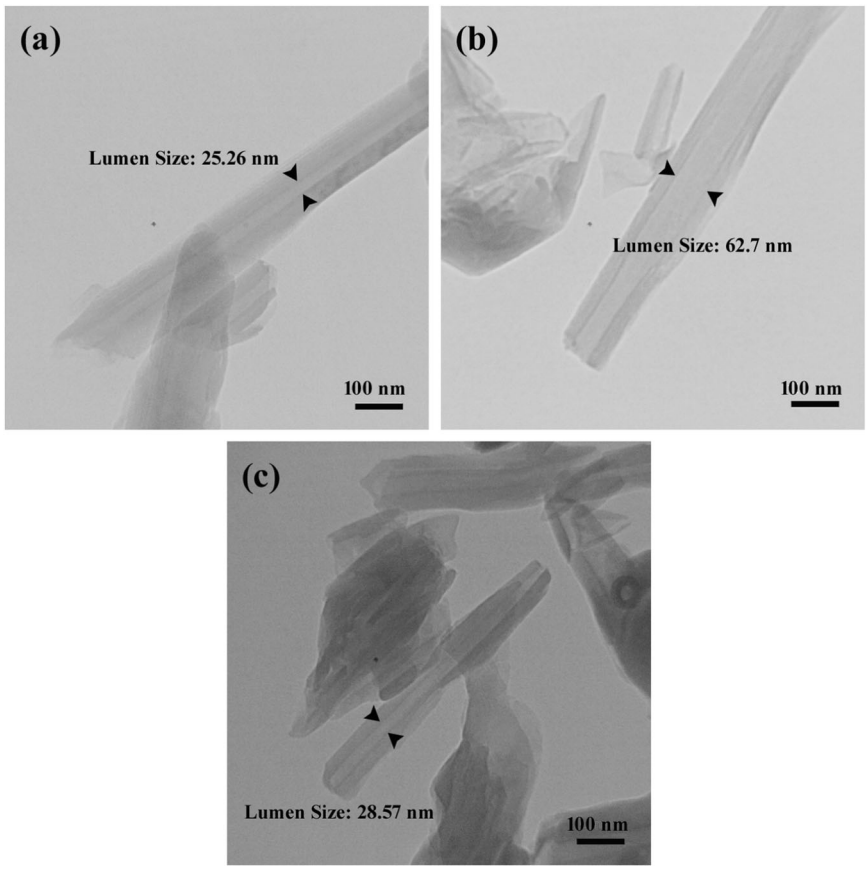

Fig. 5 TEM images of **a** HNT, **b**, EHNT, and **c** CHNT

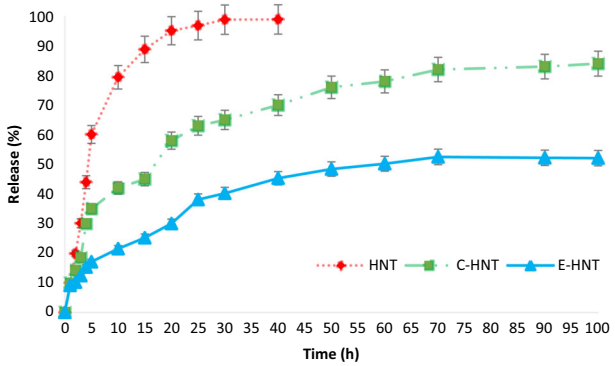

Fig. 6 Release profiles of LOS from the HNTs, CHNTs, and EHNTs in phosphate buffer solution (pH = 7.4.) Data are presented as means ± SD ($n = 3$)

CHNT ($p < 0.05$). LOS could release rapidly from LOS-loaded HNT and the release reached 95% in 20 h, which was ascribed to hydrophilic characteristic of HNTs and good solubility of LOS in pH 7.4 phosphate buffer solution. The release rate from LOS-loaded CHNT and LOS-loaded EHNT notably decelerated. Only 42 and 21.5% of LOS released from CHNT and EHNT in the first 10 h, respectively, and the release rate gradually increased to ~ 76% in 50 h for CHNT. In comparison with that from CHNT, the release rate of LOS further reduced in EHNT. A nearly constant release of LOS was obtained from EHNT, the release rate only increased to 52.5% in 70 h.

Three kinetics (Higuchi, first order, and power law) models usually used to explain the release of guest molecules from porous substrates, were used to simulate the release of LOS from HNTs. The release profiles of LOS from HNT samples were fitted using the above models. Moreover, the values of correlation coefficient (R^2) and the release parameter values were shown in Table 2.

The R^2 of power law kinetic model were larger than those of other models. It was found that the release of LOS from the all HNTs samples (HNTs, CHNTs, and EHNTs) were controlled by a drug diffusion process or Fickian diffusion ($n = 0.48$, 0.45, and 0.43 for HNTs, CHNTs, and EHNTs, respectively). It could be concluded that the LOS molecules are released from the HNT inner lumen by a diffusion process. The calculated diffusional exponents (0.48 and 0.43) vary slightly from expected value (0.45) for Fickian diffusion. This difference is owing to the experimental condition not fully satisfying the assumption of the power model (an ideal geometry, uniform conditions, and a single release mechanism, etc.) (Yuan et al. 2012).

Table 2 Parameters of the three fitting models of LOS-loaded halloysite samples

Samples	Power law			First order		Higuchi's model		
	k_p	n	R^2	k_1	R^2	k_H	b	R^2
HNTs	1.349	0.48	0.9205	0.044	0.5517	1.766	0.673	0.8671
CHNTs	1.184	0.45	0.9407	0.016	0.5764	0.839	1.173	0.9234
EHNTs	0.803	0.43	0.9815	0.016	0.6998	0.547	0.533	0.9473

Conclusions

In this work, a simple and effective method was used for sustained release of LOS as a high blood pressure–controller drug using HNTs. HNTs are natural materials that are categorized in kaolin group, so this work can be considered as eco-friendly method that is compatible, safe, and appropriate for drug-delivery systems. Herein, HNTs were improved by two processes: calcination and etching, and the effect of them on characteristics of HNT was studied. The results showed that activation of HNTs through calcination and etching processes can be effective on drug-loading amount and release rate of it. However, whereas etching process increased both the BET-specific surface area and drug-loading amount, the calcination process only increased the surface area and decreased drug-loading amount, because of removal of water molecules that play key role in loading step. Therefore, EHNT loaded the maximum amount of LOS and CHNT loaded the minimum amount of it. According to the findings, lumen sizes of HNTs were changed by the activation processes, but they had no effect on morphology and structure of HNTs. Release rate of drug from various HNTs was investigated and it was concluded that maximum and minimum release rate of LOS are assigned to simple HNT and EHNT, respectively. It was found that, the lumen size is not the only parameter on loading amount and the other parameters such as water molecules can also be effective on it. Kinetics studies confirmed that releasing the LOS molecules from HNTs followed by diffusion process is identified as Fickian diffusion.

Acknowledgements This study was funded by the Islamic Azad University, Bandar Abbas Branch, Iran by Grant No (9570/59008).

Compliance with ethical standards

Conflict of interest The authors declare that they have no conflict of interest.

References

Abdullayev E, Joshi A, Wei W, Zhao Y, Lvov Y (2012) Enlargement of halloysite clay nanotube lumen by selective etching of aluminum oxide. ACS Nano 6:7216–7226

Alavi M, Karimi N, Safaei M (2017) Application of various types of liposomes in drug delivery systems. Adv Pharm Bull 7:3–9

Baeza A, Ruiz-Molina D, Vallet-Regí M (2017) Recent advances in porous nanoparticles for drug delivery in antitumoral applications: inorganic nanoparticles and nanoscale metal-organic frameworks. Expert Opin Drug Deliv 14:783–796

Callender SP, Mathews JA, Kobernyk K, Wettig SD (2017) Microemulsion utility in pharmaceuticals: implications for multi-druag delivery. Int J Pharm 526:425–442

Cavallaro G, Lazzara G, Massaro M, Milioto S, Noto R, Parisi F, Riela S (2015) Biocompatible poly (N-isopropylacrylamide)-halloysite nanotubes for thermoresponsive curcumin release. J Phys Chem C 119:8944–8951

Cavallaro G, Lazzara G, Milioto S (2012) Exploiting the colloidal stability and solubilization ability of clay nanotubes/ionic surfactant hybrid nanomaterials. J Phys Chem C 116:21932–21938

Cavallaro G, Lazzara G, Milioto S, Parisi F, Sanzillo V (2013) Modified halloysite nanotubes: nanoarchitectures for enhancing the capture of oils from vapor and liquid phases. ACS Appl Mater Inter 6:606–612

Chithaluru K, Tadikonda R, Gollapudi R, Kandula KKK (2011) Formulation and invitro evaluation of sustained release matrix tablets of losartan potassium. Cellulose 1200:200

Groen JC, Peffer LA, Pérez-Ramírez J (2003) Pore size determination in modified micro-and mesoporous materials. Pitfalls and limitations in gas adsorption data analysis. Micropor Mesopor Mat 60:1–17

Hemmatpour H, Haddadi-Asl V, Roghani-Mamaqani H (2015) Synthesis of pH-sensitive poly (N,N-dimethylaminoethylmethacrylate)-grafted halloysite nanotubes for adsorption and controlled release of DPH and DS drugs. Polymer 65:143–153

Hoffman AS (2008) The origins and evolution of "controlled" drug delivery systems. J Control Release 132:153–163

Ibrahim MM (2015) Investigation on thermal stability and purity determination of two antihypertensive drugs, valsartan and losartan potassium. Int J Curr Pharm Res 7:64–69

Kadam AA, Jang J, Lee DS (2017) Supermagnetically tuned halloysite nanotubes functionalized with aminosilane for covalent laccase immobilization. ACS Appl Mater Interf 9:15492–15501

Kadi S, Lellou S, Marouf-Khelifa K, Schott J, Gener-Batonneau I, Khelifa A (2012) Preparation, characterisation and application of thermally treated Algerian halloysite. Micropor Mesopor Mat 158:47–54

Kerdsakundee N, Li W, Martins JP, Liu Z, Zhang F, Kemell M, Correia A, Ding Y, Airavaara M, Hirvonen J (2017) Multifunctional nanotube–mucoadhesive poly (methyl vinyl ether-co-maleic acid)@ hydroxypropyl methylcellulose acetate succinate composite for site-specific oral drug delivery. Adv Healthcare Mater 6:1700629–1700641

Li H, Zhu X, Zhou H, Zhong S (2015) Functionalization of halloysite nanotubes by enlargement and hydrophobicity for sustained release of analgesic. Colloid Surf A 487:154–161

Lvov Y, Abdullayev E (2013) Functional polymer–clay nanotube composites with sustained release of chemical agents. Prog Polym Sci 38:1690–1719

Lvov YM, Shchukin DG, Mohwald H, Price RR (2008) Halloysite clay nanotubes for controlled release of protective agents. ACS Nano 2:814–820

Mokale V, Jitendra N, Yogesh S, Gokul K (2014) Chitosan reinforced alginate controlled release beads of losartan potassium: design, formulation and in vitro evaluation. J Pharm Investig 44:243–252

Mu B, Zhao MF, Liu P (2008) Halloysite nanotubes grafted hyperbranched (co) polymers via surface-initiated self-condensing vinyl (co) polymerization. J Nanopart Res 10:831–838

Nicolini KP, Fukamachi CRB, Wypych F, Mangrich AS (2009) Dehydrated halloysite intercalated mechanochemically with urea: thermal behavior and structural aspects. J Colloid Interface Sci 338:474–479

Nie J, Cheng W, Peng Y, Liu G, Chen Y, Wang X, Liang C, Tao W, Wei Y, Zeng X (2017) Co-delivery of docetaxel and bortezomib based on a targeting nanoplatform for enhancing cancer chemotherapy effects. Drug Deliv 24:1124–1138

Pan J, Yao H, Xu L, Ou H, Huo P, Li X, Yan Y (2011) Selective recognition of 2,4,6-trichlorophenol by molecularly imprinted polymers based on magnetic halloysite nanotubes composites. J Phys Chem C 115:5440–5449

Pan J, Zhu W, Dai X, Yan X, Gan M, Li L, Hang H, Yan Y (2014) Magnetic molecularly imprinted microcapsules derived from pickering emulsion polymerization and their novel adsorption characteristics for λ-cyhalothrin. RSC Adv 4:4435–4443

Patel K (2010) Once-daily sustained-release matrix tablets of losartan potassium: formulation and in vitro evaluation. Int J Med Clin Res 1:1–7

Raju DB, Suresh John K, Varma MM (2010) Formulation and evaluation of losartan potassium matrix tablets for oral controlled release. J Chem Pharm Res 2:130–135

Sarwar S, Hossain MS (2012) Development and evaluation of sustained release losartan potassium matrix tablet using kollidon SR as release retardant. Braz J Pharm Sci 48:621–628

Tan D, Yuan P, Annabi-Bergaya F, Yu H, Liu D, Liu H, He H (2013) Natural halloysite nanotubes as mesoporous carriers for the loading of ibuprofen. Micropor Mesopor Mat 179:89–98

Vergaro V, Abdullayev E, Lvov YM, Zeitoun A, Cingolani R, Rinaldi R, Leporatti S (2010) Cytocompatibility and uptake of halloysite clay nanotubes. Biomacromolecules 11:820–826

Vergaro V, Lvov YM, Leporatti S (2012) Halloysite clay nanotubes for resveratrol delivery to cancer cells. Macromol Biosci 12:1265–1271

Viseras M, Aguzzi C, Cerezo P, Viseras C, Valenzuela C (2008) Equilibrium and kinetics of 5-aminosalicylic acid adsorption by halloysite. Micropor Mesopor Mat 108:112–116

Wang Q, Zhang J, Zheng Y, Wang A (2014) Adsorption and release of ofloxacin from acid-and heat-treated halloysite. Colloid Surf B 113:51–58

Wei W, Minullina R, Abdullayev E, Fakhrullin R, Mills D, Lvov Y (2014) Enhanced efficiency of antiseptics with sustained release from clay nanotubes. RSC Adv 4:488–494

White RD, Bavykin DV, Walsh FC (2012) The stability of halloysite nanotubes in acidic and alkaline aqueous suspensions. Nanotechnology 23:065705

Xin Y, Huang Q, Tang JQ, Hou XY, Zhang P, Zhang LZ, Jiang G (2016) Nanoscale drug delivery for targeted chemotherapy. Cancer Lett 379:24–31

Xin Y, Yin M, Zhao L, Meng F, Luo L (2017) Recent progress on nanoparticle-based drug delivery systems for cancer therapy. Cancer Biol Med 14:228–241

Yah WO, Takahara A, Lvov YM (2012) Selective modification of halloysite lumen with octadecylphosphonic acid: new inorganic tubular micelle. J Am Chem Soc 134:1853–1859

Yuan P, Southon PD, Liu Z, Kepert CJ (2012) Organosilane functionalization of halloysite nanotubes for enhanced loading and controlled release. Nanotechnology 23:375705

Zhang AB, Pan L, Zhang HY, Liu ST, Ye Y, Xia MS, Chen XG (2012) Effects of acid treatment on the physico-chemical and pore characteristics of halloysite. Colloid Surf A 396:182–188

Zhang RX, Ahmed T, Li LY, Li J, Abbasi AZ, Wu XY (2017) Design of nanocarriers for nanoscale drug delivery to enhance cancer treatment using hybrid polymer and lipid building blocks. Nanoscale 9:1334–1355